

# Channel Estimation for Wireless OFDM Communications

Jia-Chin Lin  
*National Central University*  
*Taiwan*

## 1. Introduction

### 1.1 Preliminary

Orthogonal frequency-division multiplexing (OFDM) communication techniques have recently received significant research attention because of their ability to maintain effective transmission and highly efficient bandwidth utilization in the presence of various channel impairments, such as severely frequency-selective channel fades caused by long multipath delay spreads and impulsive noise (Bingham, 1990; Zou & Wu, 1995). In an OFDM system, a high-rate serial information-bearing symbol stream is split into many low-rate parallel streams; each of these streams individually modulates a mutually orthogonal sub-carrier. The spectrum of an individual sub-channel overlaps with those expanded from the adjacent sub-channels. However, the OFDM sub-carriers are orthogonal as long as they are synthesized such that the frequency separation between any two adjacent sub-carriers is exactly equal to the reciprocal of an OFDM block duration. A discrete Fourier transform (DFT) operation can perfectly produce this sub-carrier arrangement and its relevant modulations (Darlington, 1970; Weinstein & Ebert, 1971). Because of the advanced technologies incorporated into integrated circuit (IC) chips and digital signal processors (DSPs), OFDM has become a practical way to implement very effective modulation techniques for various applications. As a result, OFDM technologies have recently been chosen as candidates for 4th-generation (4G) mobile communications in a variety of standards, such as IEEE 802.16 (Marks, 2008) and IEEE 802.20 (Klerer, 2005) in the United States, and international research projects, such as EU-IST-MATRICE (MATRICE, 2005) and EU-IST-4MORE (4MORE, 2005) for 4G mobile communication standardization in Europe. Regarding the history of OFDM, recall that Chang published a paper on the synthesis of band-limited signals for parallel multi-channel transmission in the 1960s (Chang, 1966). The author investigated a technique for transmitting and receiving (transceiving) parallel information through a linear band-limited channel without inter-channel interference (ICI) or inter-symbol interference (ISI). Saltzberg then conducted relevant performance evaluations and analyses (Saltzberg, 1967).

### 1.2 IFFT and FFT utilization: A/D realization of OFDM

A significant breakthrough in OFDM applicability was presented by Weinstein and Ebert in 1971 (Weinstein & Ebert, 1971). First, DFT and inverse DFT (IDFT) techniques were applied

Source: Communications and Networking, Book edited by: Jun Peng,  
ISBN 978-953-307-114-5, pp. 434, September 2010, Sciyo, Croatia, downloaded from SCIYO.COM

to OFDM implementation to perform base-band parallel sub-channel modulations and demodulations (or multiplexing and demultiplexing) (Weinstein & Ebert, 1971). This study provided an effective discrete-time signal processing method to simultaneously modulate (and demodulate) signals transmitted (and received) on various sub-channels without requiring the implementation of a bank of sub-carrier modulators with many analog multipliers and oscillators. Meanwhile, ISI can be significantly reduced by inserting a guard time-interval (GI) in between any two consecutive OFDM symbols and by applying a raised-cosine windowing method to the time-domain (TD) signals (Weinstein & Ebert, 1971). Although the system studied in this work cannot always maintain orthogonality among sub-carriers when operated over a time-dispersive channel, the application of IDFT and DFT to OFDM communication is not only a crucial contribution but also a critical driving force for commercial applicability of recent wireless OFDM communication because the fast algorithms of IDFT and DFT, i.e., inverse fast Fourier transform (IFFT) and fast Fourier transform (FFT), have been commercialized and popularly implemented with ASICs or sub-functions on DSPs.

### 1.3 Cyclic prefix

Orthogonality among sub-carriers cannot be maintained when an OFDM system operates over a time-dispersive channel. This problem was first addressed by Peled and Ruiz in 1980 (Peled & Ruiz, 1980). Rather than inserting a blank GI between any two consecutive OFDM symbols, which was the method employed in the previous study (Weinstein & Ebert, 1971), a cyclic extension of an OFDM block is inserted into the original GI as a prefix to an information-bearing OFDM block. The adopted cyclic prefix (CP) effectively converts the linear convolution of the transmitted symbol and the channel impulse response (CIR) into the cyclic convolution; thus, orthogonality among sub-carriers can be maintained with channel time-dispersion if the CP is sufficiently longer than the CIR. However, energy efficiency is inevitably sacrificed, as the CPs convey no desired information.

### 1.4 Applications

OFDM technology is currently employed in the European digital audio broadcasting (DAB) standard (DAB, 1995). In addition, digital TV broadcasting applications based on OFDM technology have been under comprehensive investigation (DVB, 1996; Couasnon et al., 1994; Marti et al., 1993; Moeneclaey & Bladel, 1993; Tourtier et al., 1993). Furthermore, OFDM technology in conjunction with other multiple-access techniques, in particular code-division multiple-access (CDMA) techniques, for mobile communications has also been the focus of a variety of research efforts (Hara & Prasad, 1997; Sourour & Nakagawa, 1996; Kondo & Milstein, 1996; Reiners & Rohling, 1994; Fazel, 1994). For those employed in wireline environments, OFDM communication systems are often called "Discrete Multi-Tone" (DMT) communications, which have also attracted a great deal of research attention as a technology that effectively achieves high-rate transmission on currently existing telephone networks (Bingham, 1990; Young et al., 1996; Chow, 1993; Tu, 1991). One of the major advantages of the OFDM technique is its robustness with multipath reception. OFDM applications often are expected to operate in a severely frequency-selective environment. Therefore, OFDM communication has recently been selected for various broadband mobile communications, e.g., 4G mobile communications. This chapter will focus on such applications.

### 1.5 System description and signal modelling

The primary idea behind OFDM communication is dividing an occupied frequency band into many parallel sub-channels to deliver information simultaneously. By maintaining sufficiently narrow sub-channel bandwidths, the signal propagating through an individual sub-channel experiences roughly frequency-flat (i.e., frequency-nonselective) channel fades. This arrangement can significantly reduce the complexity of the subsequent equalization sub-system. In particular, current broadband wireless communications are expected to be able to operate in severe multipath fading environments in which long delay spreads inherently exist because the signature/chip duration has become increasingly shorter. To enhance spectral (or bandwidth) efficiency, the spectra of adjacent sub-channels are set to overlap with one another. Meanwhile, the orthogonality among sub-carriers is maintained by setting the sub-carrier spacing (i.e., the frequency separation between two consecutive sub-carriers) to the reciprocal of an OFDM block duration.

By taking advantage of a CP, the orthogonality can be prevented from experiencing ICI even for transmission over a multipath channel (Peled & Ruiz, 1980). Although several variants of OFDM communication systems exist (Bingham, 1990; Weinstein & Ebert, 1971; Floch et al., 1995), CP-OFDM (Peled & Ruiz, 1980) is primarily considered in this section due to its popularity. A CP is obtained from the tail portion of an OFDM block and then prefixed into a transmitted block, as shown in Fig. 1.

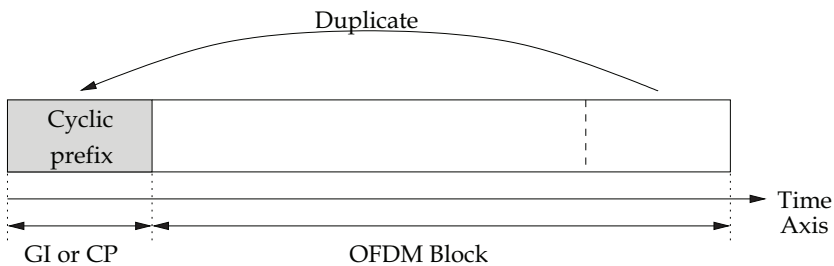


Fig. 1. An OFDM symbol consisting of a CP and an information-bearing OFDM block.

A portion of the transmitted OFDM symbol becomes periodic. The CP insertion converts the linear convolution of the CIR and the transmitted symbol into the circular convolution of the two. Therefore, CPs can avoid both ISI and ICI (Bingham, 1990). In this fundamental section, the following assumptions are made for simplicity: (1) a cyclic prefix is used; (2) the CIR length does not exceed the CP length; (3) the received signal can be perfectly synchronized; (4) noise is complex-valued, additive, white Gaussian noise (AWGN); and (5) channel time-variation is slow, so the channel can be considered to be constant or static within a few OFDM symbols.

#### 1.5.1 Continuous-time model

A continuous-time base-band equivalent representation of an OFDM transceiver is depicted in Fig. 2. The OFDM communication system under study consists of  $N$  sub-carriers that occupy a total bandwidth of  $B = \frac{1}{T_s}$  Hz. The length of an OFDM symbol is set to  $T_{sym}$  seconds; moreover, an OFDM symbol is composed of an OFDM block of length  $T = NT_s$  and a CP of length  $T_g$ . The transmitting filter on the  $k$ th sub-carrier can be written as

$$p_k(t) = \begin{cases} \frac{1}{\sqrt{T}} e^{j2\pi \frac{B}{N} k(t-T_g)} & 0 \leq t \leq T_{sym} \\ 0 & \text{otherwise,} \end{cases} \quad (1)$$

where  $T_{sym} = T + T_g$ . Note that  $p_k(t) = p_k(t+ T)$  when  $t$  is within the guard interval  $[0, T_g]$ . It can be seen from Equation 1 that  $p_k(t)$  is a rectangular pulse modulated by a sub-carrier with frequency  $k \cdot \frac{B}{N}$ . The transmitted signal  $s_i(t)$  for the  $i$ th OFDM symbol can thus be obtained by summing over all modulated signals, i.e.,

$$s_i(t) = \sum_{k=0}^{N-1} X_{k,i} p_k(t - iT_{sym}), \quad (2)$$

where  $X_{0,i}, X_{1,i}, \dots, X_{N-1,i}$  are complex-valued information-bearing symbols, whose values are often mapped according to quaternary phase-shift keying (QPSK) or quadrature amplitude modulation (QAM). Therefore, the transmitted signal  $s(t)$  can be considered to be a sequence of OFDM symbols, i.e.,

$$s(t) = \sum_{i=-\infty}^{\infty} s_i(t) = \sum_{i=-\infty}^{\infty} \sum_{k=0}^{N-1} X_{k,i} p_k(t - iT_{sym}). \quad (3)$$

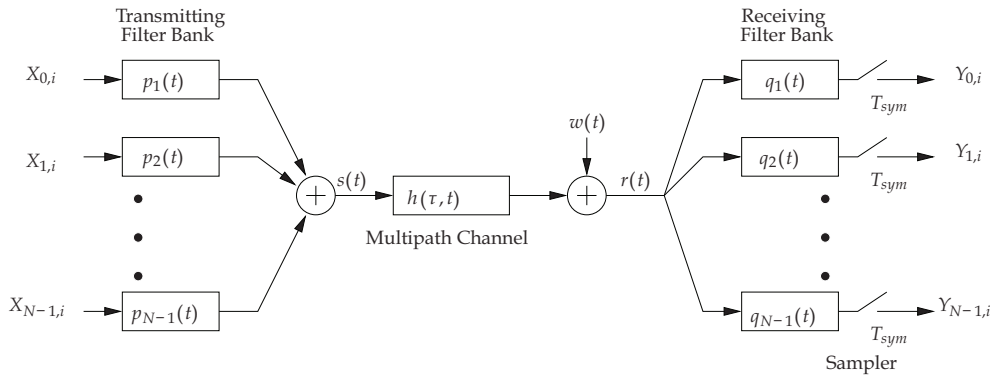


Fig. 2. Continuous-time base-band equivalent representation of an OFDM transceiver.

If the length of the CIR  $h(\tau, t)$  does not exceed the CP length  $T_g$ , the received signal  $r(t)$  can be written as

$$r(t) = (h * s)(t) + w(t) = \int_0^{T_g} h(\tau, t) s(t - \tau) d\tau + w(t), \quad (4)$$

where the operator “\*” represents the linear convolution and  $w(t)$  is an AWGN.

At the receiving end, a bank of filters is employed to match the last part  $[T_g, T_{sym}]$  of the transmitted waveforms  $p_k(t)$  on a subchannel-by-subchannel basis. By taking advantage of

matched filter (MF) theory, the receiving filter on the  $k$ th sub-channel can be designed to have the following impulse response:

$$q_k(t) = \begin{cases} p_k^*(T_{sym} - t), & 0 \leq t < T = T_{sym} - T_g \\ 0, & \text{otherwise.} \end{cases} \tag{5}$$

Because the CP can effectively separate symbol dispersion from preceding or succeeding symbols, the sampled outputs of the receiving filter bank convey negligible ISI. The time index  $i$  can be dropped for simplicity because the following derivations address the received signals on a symbol-by-symbol basis and the ISI is considered to be negligible. Using Equations 3, 4 and 5, the sampled output of the  $k$ th receiving MF can be written as

$$\begin{aligned} Y_k &= (r * q_k)(t) \Big|_{t=T_{sym}} \\ &= \int_{-\infty}^{\infty} r(\zeta) q_k(T_{sym} - \zeta) d\zeta \\ &= \int_{T_g}^{T_{sym}} \left( \int_0^{T_g} h(\tau, t) s(\zeta - \tau) d\tau + w(\zeta) \right) p_k^*(\zeta) d\zeta \\ &= \int_{T_g}^{T_{sym}} \left( \int_0^{T_g} h(\tau, t) \left[ \sum_{l=0}^{N-1} X_l p_l(\zeta - \tau) \right] d\tau \right) p_k^*(\zeta) d\zeta + \int_{T_g}^{T_{sym}} w(\zeta) p_k^*(\zeta) d\zeta. \end{aligned} \tag{6}$$

It is assumed that although the CIR is time-varying, it does not significantly change within a few OFDM symbols. Therefore, the CIR can be further represented as  $h(\tau)$ . Equation 6 can thus be rewritten as

$$Y_k = \sum_{l=0}^{N-1} X_l \int_{T_g}^{T_{sym}} \left( \int_0^{T_g} h(\tau) p_l(\zeta - \tau) d\tau \right) p_k^*(\zeta) d\zeta + \int_{T_g}^{T_{sym}} w(\zeta) p_k^*(\zeta) d\zeta. \tag{7}$$

From Equation 7, if  $T_g < \zeta < T_{sym}$  and  $0 < \tau < T_g$ , then  $0 < \zeta - \tau < T_{sym}$ . Therefore, by substituting Equation 1 into Equation 7, the inner-most integral of Equation 7 can be reformulated as

$$\begin{aligned} \int_0^{T_g} h(\tau) p_l(\zeta - \tau) d\tau &= \int_0^{T_g} h(\tau) \frac{e^{j2\pi l(\zeta - \tau - T_g)B/N}}{\sqrt{T}} d\tau \\ &= \frac{e^{j2\pi l(\zeta - T_g)B/N}}{\sqrt{T}} \int_0^{T_g} h(\tau) e^{-j2\pi l\tau B/N} d\tau, \quad T_g < \zeta < T_{sym}. \end{aligned} \tag{8}$$

Furthermore, the integration in Equation 8 can be considered to be the channel weight of the  $l$ th sub-channel, whose sub-carrier frequency is  $f = lB/N$ , i.e.,

$$H_l = H \left( l \frac{B}{N} \right) = \int_0^{T_g} h(\tau) e^{-j2\pi l\tau B/N} d\tau, \tag{9}$$

where  $H(f)$  denotes the channel transfer function (CTF) and is thus the Fourier transform of  $h(\tau)$ . The output of the  $k$ th receiving MF can therefore be rewritten as

$$\begin{aligned}
 Y_k &= \sum_{l=0}^{N-1} X_l \int_{T_g}^{T_{sym}} \frac{e^{j2\pi l(\zeta-T_g)B/N}}{\sqrt{T}} H_l p_k^*(\zeta) d\zeta + \int_{T_g}^{T_{sym}} w(\zeta) p_k^*(\zeta) d\zeta \\
 &= \sum_{l=0}^{N-1} X_l H_l \int_{T_g}^{T_{sym}} p_l(\zeta) p_k^*(\zeta) d\zeta + W_k,
 \end{aligned}
 \tag{10}$$

where

$$W_k = \int_{T_g}^{T_{sym}} w(\zeta) p_k^*(\zeta) d\zeta.$$

The transmitting filters  $p_k(t)$ ,  $k = 0, 1, \dots, N - 1$  employed here are mutually orthogonal, i.e.,

$$\begin{aligned}
 \int_{T_g}^{T_{sym}} p_l(t) p_k^*(t) dt &= \int_{T_g}^{T_{sym}} \frac{e^{j2\pi l(t-T_g)B/N}}{\sqrt{T}} \frac{e^{-j2\pi k(t-T_g)B/N}}{\sqrt{T}} dt \\
 &= \delta[k - l],
 \end{aligned}
 \tag{11}$$

where

$$\delta[k - l] = \begin{cases} 1 & k = l \\ 0 & \text{otherwise} \end{cases}$$

is the Kronecker delta function. Therefore, Equation 10 can be reformulated as

$$Y_k = H_k X_k + W_k, \quad k = 0, 1, \dots, N - 1,
 \tag{12}$$

where  $W_k$  is the AWGN of the  $k$ th sub-channel. As a result, the OFDM communication system can be considered to be a set of parallel frequency-flat (frequency-nonselective) fading sub-channels with uncorrelated noise, as depicted in Fig. 3.

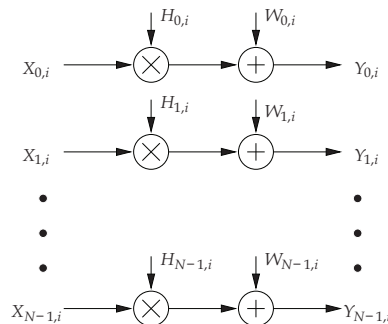


Fig. 3. OFDM communication is converted to transmission over parallel frequency-flat sub-channels.

### 1.5.2 Discrete-time model

A fully discrete-time representation of the OFDM communication system studied here is depicted in Fig. 4. The modulation and demodulation operations in the continuous-time model have been replaced by IDFT and DFT operations, respectively, and the channel has been replaced by a discrete-time channel.

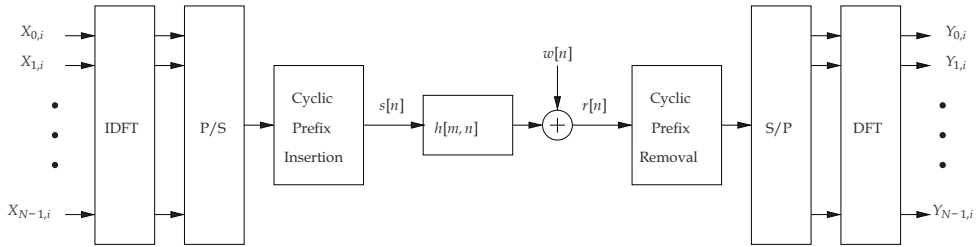


Fig. 4. Discrete-time representation of a base-band equivalent OFDM communication system.

If the CP is longer than the CIR, then the linear convolution operation can be converted to a cyclic convolution. The cyclic convolution is denoted as ‘ $\otimes$ ’ in this chapter. The  $i$ th block of the received signals can be written as

$$\begin{aligned} \mathbf{Y}_i &= \text{DFT}_N \{ \text{IDFT}_N \{ \mathbf{X}_i \} \otimes \mathbf{h}_i + \mathbf{w}_i \} \\ &= \text{DFT}_N \{ \text{IDFT}_N \{ \mathbf{X}_i \} \otimes \mathbf{h}_i \} + \mathbf{W}_i, \end{aligned} \tag{13}$$

where  $\mathbf{Y}_i = [Y_{0,i} \ Y_{1,i} \ \dots \ Y_{N-1,i}]^T$  is an  $N \times 1$  vector, and its elements represent  $N$  demodulated symbols;  $\mathbf{X}_i = [X_{0,i} \ X_{1,i} \ \dots \ X_{N-1,i}]^T$  is an  $N \times 1$  vector, and its elements represent  $N$  transmitted information-bearing symbols;  $\mathbf{h}_i = [h_{0,i} \ h_{1,i} \ \dots \ h_{N-1,i}]^T$  is an  $N \times 1$  vector, and its elements represent the CIR padded with sufficient zeros to have  $N$  dimensions; and  $\mathbf{w}_i = [w_{0,i} \ w_{1,i} \ \dots \ w_{N-1,i}]^T$  is an  $N \times 1$  vector representing noise. Because the noise is assumed to be white, Gaussian and circularly symmetric, the noise term

$$\mathbf{W}_i = \text{DFT}_N(\mathbf{w}_i) \tag{14}$$

represents uncorrelated Gaussian noise, and  $W_{k,i}$  and  $w_{n,i}$  can be proven to have the same variance according to the Central Limit Theorem (CLT). Furthermore, if a new operator “ $\odot$ ” is defined to be element-by-element multiplication, Equation 13 can be rewritten as

$$\begin{aligned} \mathbf{Y}_i &= \mathbf{X}_i \odot \text{DFT}_N \{ \mathbf{h}_i \} + \mathbf{W}_i \\ &= \mathbf{X}_i \odot \mathbf{H}_i + \mathbf{W}_i, \end{aligned} \tag{15}$$

where  $\mathbf{H}_i = \text{DFT}_N \{ \mathbf{h}_i \}$  is the CTF. As a result, the same set of parallel frequency-flat sub-channels with noise as presented in the continuous-time model can be obtained.

Both the aforementioned continuous-time and discrete-time representations provide insight and serve the purpose of providing a friendly first step or entrance point for beginning readers. In my personal opinion, researchers that have more experience in communication fields may be more comfortable with the continuous-time model because summations, integrations and convolutions are employed in the modulation, demodulation and (CIR)

filtering processes. Meanwhile, researchers that have more experience in signal processing fields may be more comfortable with the discrete-time model because vector and matrix operations are employed in the modulation, demodulation and (CIR) filtering processes. Although the discrete-time model may look neat, clear and reader-friendly, several presumptions should be noted and kept in mind. It is assumed that the symbol shaping is rectangular and that the frequency offset, ISI and ICI are negligible. The primary goal of this chapter is to highlight concepts and provide insight to beginning researchers and practical engineers rather than covering theories or theorems. As a result, the derivations shown in Sections 3 and 4 are close to the continuous-time representation, and those in Sections 5 and 6 are derived from the discrete-time representation.

## 2. Introduction to channel estimation on wireless OFDM communications

### 2.1 Preliminary

In practice, effective channel estimation (CE) techniques for coherent OFDM communications are highly desired for demodulating or detecting received signals, improving system performance and tracking time-varying multipath channels, especially for mobile OFDM because these techniques often operate in environments where signal reception is inevitably accompanied by wide Doppler spreads caused by dynamic surroundings and long multipath delay spreads caused by time-dispersion. Significant research efforts have focused on addressing various CE and subsequent equalization problems by estimating sub-channel gains or the CIR. CE techniques in OFDM systems often exploit several pilot symbols transceived at given locations on the frequency-time grid to determine the relevant channel parameters. Several previous studies have investigated the performance of CE techniques assisted by various allocation patterns of the pilot/training symbols (Coleri et al., 2002; Li et al., 2002; Yeh & Lin, 1999; Negi & Cioffi, 1998). Meanwhile, several prior CEs have simultaneously exploited both time-directional and frequency-directional correlations in the channel under investigation (Hoeher et al., 1997; Wilson et al., 1994; Hoeher, 1991). In practice, these two-dimensional (2D) estimators require 2D Wiener filters and are often too complicated to be implemented. Moreover, it is difficult to achieve any improvements by using a 2D estimator, while significant computational complexity is added (Sandell & Edfors, 1996). As a result, serially exploiting the correlation properties in the time and frequency directions may be preferred (Hoeher, 1991) for reduced complexity and good estimation performance. In mobile environments, channel tap-weighting coefficients often change rapidly. Thus, the comb-type pilot pattern, in which pilot symbols are inserted and continuously transmitted over specific pilot sub-channels in all OFDM blocks, is naturally preferred and highly desirable for effectively and accurately tracking channel time-variations (Negi & Cioffi, 1998; Wilson et al., 1994; Hoeher, 1991; Hsieh & Wei, 1998).

Several methods for allocating pilots on the time-frequency grid have been studied (Tufvesson & Maseng, 1997). Two primary pilot assignments are depicted in Fig. 5: the block-type pilot arrangement (BTPA), shown in Fig. 5(a), and the comb-type pilot arrangement (CTPA), shown in Fig. 5(b). In the BTPA, pilot signals are assigned in specific OFDM blocks to occupy all sub-channels and are transmitted periodically. Both in general and in theory, BTPA is more suitable in a slowly time-varying, but severely frequency-selective fading environment. No interpolation method in the FD is required because the pilot block occupies the whole band. As a result, the BTPA is relatively insensitive to severe

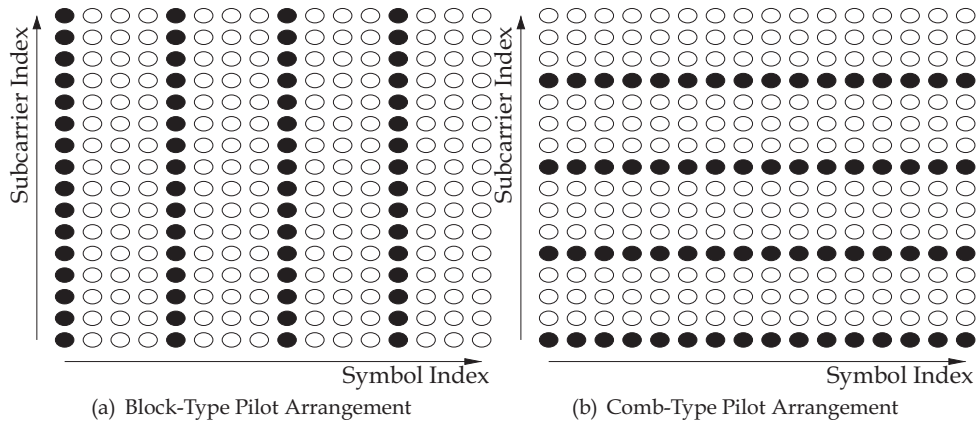


Fig. 5. Two primary pilot assignment methods

frequency selectivity in a multipath fading channel. Estimates of the CIR can usually be obtained by least-squares (LS) or minimum-mean-square-error (MMSE) estimations conducted with assistance from the pilot symbols (Edfors et al., 1996; Van de Beek et al., 1995).

In the CTPA, pilot symbols are often uniformly distributed over all sub-channels in each OFDM symbol. Therefore, the CTPA can provide better resistance to channel time-variations. Channel weights on non-pilot (data) sub-channels have to be estimated by interpolating or smoothing the estimates of the channel weights obtained on the pilot sub-channels (Zhao & Huang, 1997; Rinne & Renfors, 1996). Therefore, the CTPA is, both in general and in theory, sensitive to the frequency-selectivity of a multipath fading channel. The CTPA is adopted to assist the CE conducted in each OFDM block in Sections 3 and 4, while the BTPA is discussed in Section 5.

## 2.2 CTPA-based CE

Conventional CEs assisted by comb-type pilot sub-channels are often performed completely in the frequency domain (FD) and include two steps: jointly estimating the channel gains on all pilot sub-channels and smoothing the obtained estimates to interpolate the channel gains on data (non-pilot) sub-channels. The CTPA CE technique (Hsieh & Wei, 1998) and the pilot-symbol-assisted modulation (PSAM) CE technique (Edfors et al., 1998) have been shown to be practical and applicable methods for mobile OFDM communication because their ability to track rapidly time-varying channels is much better than that of a BTPA CE technique. Several modified variants for further improvements and for complexity or rank reduction by means of singular-value-decomposition (SVD) techniques have been investigated previously (Hsieh & Wei, 1998; Edfors et al., 1998; Seller, 2004; Edfors et al., 1996; Van de Beek et al., 1995; Park et al., 2004). In addition, a more recent study has proposed improving CE performance by taking advantage of presumed slowly varying properties in the delay subspace (Simeone et al., 2004). This technique employs an intermediate step between the LS pilot sub-channel estimation step and the data sub-channel interpolation step in conventional CE approaches (Hsieh & Wei, 1998; Edfors et al., 1998; Seller, 2004; Edfors et al., 1996; Van de Beek et al., 1995; Park et al., 2004) to track the delay subspace to improve the accuracy of the pilot sub-channel estimation. However, this

technique is based on the strong assumption that the multipath delays are slowly time-varying and can easily be estimated separately from the channel gain estimation. A prior channel estimation study (Minn & Bhargava, 2000) also exploited CTPA and TD CE. The proposed technique (Minn & Bhargava, 2000) was called the Frequency-Pilot-Time-Average (FPTA) method. However, time-averaging over a period that may be longer than the coherence time of wireless channels to suppress interference not only cannot work for wireless applications with real-time requirements but may also be impractical in a mobile channel with a short coherence time. A very successful technique that takes advantage of TD CE has been proposed (Minn & Bhargava, 1999). However, this technique focused on parameter estimation to transmit diversity using space-time coding in OFDM systems, and the parameter settings were not obtained from any recent mobile communication standards. To make fair comparisons of the CE performance and to avoid various diversity or space-time coding methods, only uncoded OFDM with no diversity is addressed in this chapter.

The CTPA is also employed as the framework of the technique studied in Sections 3 and 4 because of its effectiveness in mobile OFDM communications with rapidly time-varying, frequency-selective fading channels. A least-squares estimation (LSE) approach is performed serially on a block-by-block basis in the TD, not only to accurately estimate the CIR but also to effectively track rapid CIR variations. In fact, a generic estimator is thus executed on each OFDM block without assistance from a priori channel information (e.g., correlation functions in the frequency and/or in the time directions) and without increasing computational complexity.

Many previous studies (Edfors et al., 1998; Seller, 2004; Edfors et al., 1996; Van de Beek et al., 1995; Simeone et al., 2004) based on CTPA were derived under the assumption of perfect timing synchronization. In practice, some residual timing error within several sampling durations inevitably occurs during DFT demodulation, and this timing error leads to extra phase errors that phase-rotate demodulated symbols. Although a method that solves this problem in conventional CTPA OFDM CEs has been studied (Hsieh & Wei, 1998; Park et al., 2004), this method can work only under some special conditions (Hsieh & Wei, 1998). Compared with previous studies (Edfors et al., 1998; Seller, 2004; Edfors et al., 1996; Van de Beek et al., 1995; Simeone et al., 2004), the studied technique can be shown to achieve better resistance to residual timing errors because it does not employ a priori channel information and thus avoids the model mismatch and extra phase rotation problems that result from residual timing errors. Also, because the studied technique performs ideal data sub-channel interpolation with a domain-transformation approach, it can effectively track extra phase rotations with no phase lag.

### 2.3 BTPA-based CE

Single-carrier frequency-division multiple-access (SC-FDMA) communication was selected for the long-term evolution (LTE) specification in the third-generation partnership project (3GPP). SC-FDMA has been the focus of research and development because of its ability to maintain a low peak-to-average power ratio (PAPR), particularly in the uplink transmission, which is one of a few problems in recent 4G mobile communication standardization. Meanwhile, SC-FDMA can maintain high throughput and low equalization complexity like orthogonal frequency-division multiple access (OFDMA) (Myung et al., 2006). Moreover, SC-FDMA can be thought of as an OFDMA with DFT pre-coded or pre-spread inputs. In a SC-FDMA uplink scenario, information-bearing symbols in the TD from any individual user terminal are pre-coded (or pre-spread) with a DFT. The DFT-spread resultant symbols can

be transformed into the FD. Finally, the DFT-spread symbols are fed into an IDFT multiplexer to accomplish FDM.

Although the CTPA is commonly adopted in wireless communication applications, such as IEEE 802.11a, IEEE 802.11g, IEEE 802.16e and the EU-IST-4MORE project, the BTPA is employed in the LTE. As shown in the LTE specification, 7 symbols form a slot, and 20 slots form a frame that spans 10 ms in the LTE uplink transmission. In each slot, the 4th symbol is used to transmit a pilot symbol. Section 5 employs BTPA as the framework to completely follow the LTE specifications. A modified Kalman filter- (MKF-) based TD CE approach with fast fading channels has been proposed previously (Han et al., 2004). The MKF-based TD CE tracks channel variations by taking advantage of MKF and TD MMSE equalizers. A CE technique that also employs a Kalman filter has been proposed (Li et al., 2008). Both methods successfully address the CE with high Doppler spreads.

The demodulation reference signal adopted for CE in LTE uplink communication is generated from Zadoff-Chu (ZC) sequences. ZC sequences, which are generalized chirp-like poly-phase sequences, have some beneficial properties according to previous studies (Ng et al., 1998; Popovic, 1992). ZC sequences are also commonly used in radar applications and as synchronization signals in LTE, e.g., random access and cell search (Levanon & Mozeson, 2004; LTE, 2009). A BTPA-based CE technique is discussed in great detail in Section 5.

#### **2.4 TD-redundancy-based CE**

Although the mobile communication applications mentioned above are all based on cyclic-prefix OFDM (CP-OFDM) modulation techniques, several encouraging contributions have investigated some alternatives, e.g., zero-padded OFDM (ZP-OFDM) (Muquest et al., 2002; Muquet et al., 2000) and pseudo-random-postfix OFDM (PRP-OFDM) (Muck et al., 2006; 2005; 2003) to replace the TD redundancy with null samples or known/pre-determined sequences. It has been found that significant improvements over CP-OFDM can be realized with either ZP-OFDM or PRP-OFDM (Muquest et al., 2002; Muquet et al., 2000; Muck et al., 2006; 2005; 2003). In previous works, ZP-OFDM has been shown to maintain symbol recovery irrespective of null locations on a multipath channel (Muquest et al., 2002; Muquet et al., 2000). Meanwhile, PRP-OFDM replaces the null samples originally inserted between any two OFDM blocks in ZP-OFDM by a known sequence. Thus, the receiver can use the a priori knowledge of a fraction of transmitted blocks to accurately estimate the CIR and effectively reduce the loss of transmission rate with frequent, periodic training sequences (Muck et al., 2006; 2005; 2003). A more recent OFDM variant, called Time-Domain Synchronous OFDM (TDS-OFDM) was investigated in terrestrial broadcasting applications (Gui et al., 2009; Yang et al., 2008; Zheng & Sun, 2008; Liu & Zhang, 2007; Song et al., 2005). TDS-OFDM works similarly to the PRP-OFDM and also belongs to this category of CEs assisted by TD redundancy.

Several research efforts that address various PRP-OFDM CE and/or subsequent equalization problems have been undertaken (Muck et al., 2006; 2005; 2003; Ma et al., 2006). However, these studies were performed only in the context of a wireless local area network (WLAN), in which multipath fading and Doppler effects are not as severe as in mobile communication. In addition, the techniques studied in previous works (Muck et al., 2006; 2005; 2003; Ma et al., 2006) take advantage of a time-averaging method to replace statistical expectation operations and to suppress various kinds of interference, including inter-block interference (IBI) and ISI. However, these moving-average-based interference suppression methods investigated in the previous studies (Muck et al., 2006; 2005; 2003; Ma et al., 2006)

cannot function in the mobile environment because of rapid channel variation and real-time requirements. In fact, it is difficult to design an effective moving-average filter (or an integrate-and-dump (I/D) filter) for the previous studies (Muck et al., 2006; 2005; 2003; Ma et al., 2006) because the moving-average filter must have a sufficiently short time-averaging duration (i.e., sufficiently short I/D filter impulse response) to accommodate both the time-variant behaviors of channel tap-weighting coefficients and to keep the a priori statistics of the PRP unchanged for effective CE and must also have a sufficiently long time-averaging duration (i.e., sufficiently long I/D filter impulse response) to effectively suppress various kinds of interference and reduce AWGN.

A previous work (Ohno & Giannakis, 2002) investigated an optimum training pattern for generic block transmission over time-frequency selective channels. It has been proven that the TD training sequences must be placed with equal spacing to minimize mean-square errors. However, the work (Ohno & Giannakis, 2002) was still in the context of WLAN and broadcasting applications, and no symbol recovery method was studied. As shown in Section 6, the self-interference that occurs with symbol recovery and signal detection must be further eliminated by means of the SIC method.

### 3. Frequency-domain channel estimation based on comb-type pilot arrangement

#### 3.1 System description

The block diagram of the OFDM transceiver under study is depicted in Fig. 6. Information-bearing bits are grouped and mapped according to Gray encoding to become multi-amplitude-multi-phase symbols. After pilot symbol insertion, the block of data  $\{X_k, k = 0, 1, \dots, N-1\}$  is then fed into the IDFT (or IFFT) modulator. Thus, the modulated symbols  $\{x_n, n = 0, 1, \dots, N-1\}$  can be expressed as

$$x_n = \frac{1}{\sqrt{N}} \sum_{k=0}^{N-1} X_k e^{j2\pi kn/N}, \quad n = 0, 1, \dots, N-1, \quad (16)$$

where  $N$  is the number of sub-channels. In the above equation, it is assumed that there are no virtual sub-carriers, which provide guard bands, in the studied OFDM system. A CP is arranged in front of an OFDM symbol to avoid ISI and ICI, and the resultant symbol  $\{x_{cp,n}, n = -L, -L+1, \dots, N-1\}$  can thus be expressed as

$$x_{cp,n} = \begin{cases} x_{N+n} & n = -L, -L+1, \dots, -1 \\ x_n & n = 0, 1, \dots, N-1, \end{cases} \quad (17)$$

where  $L$  denotes the number of CP samples. The transmitted signal is then fed into a multipath fading channel with CIR  $h[m, n]$ . The received signal can thus be represented as

$$y_{cp}[n] = x_{cp}[n] \otimes h[m, n] + w[n], \quad (18)$$

where  $w[n]$  denotes the AWGN. The CIR  $h[m, n]$  can be expressed as (Steele, 1999)

$$h[m, n] = \sum_{i=0}^{M-1} \alpha_i e^{j2\pi v_i n T_s} \delta[mT_s - \tau_i], \quad (19)$$

where  $M$  denotes the number of resolvable propagation paths,  $\alpha_i$  represents the  $i$ th complex channel weight of the CIR,  $v_i$  denotes the maximum Doppler frequency on the  $i$ th resolvable propagation path,  $m$  is the index in the delay domain,  $n$  is the time index, and  $\tau_i$  denotes the delay of the  $i$ th resolvable path.

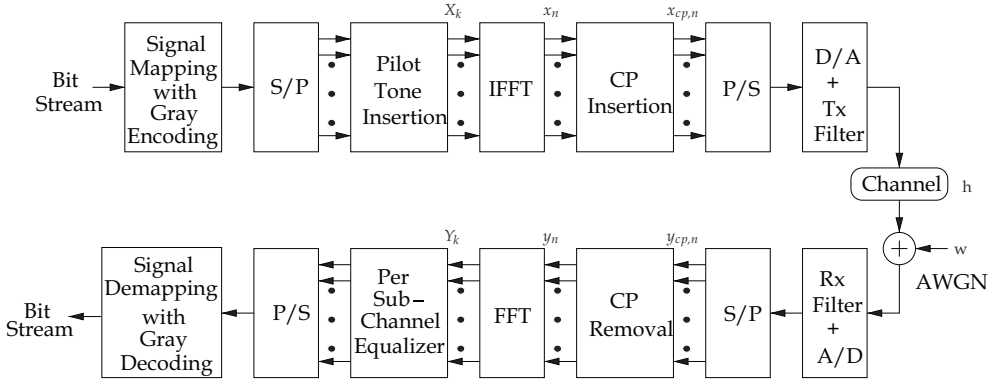


Fig. 6. A base-band equivalent block diagram of the studied OFDM transceiver.

After the CP portion is effectively removed from  $y_{cp,n}$ , the received samples  $y_n$  are sifted and fed into the DFT demodulator to simultaneously demodulate the signals propagating through the multiple sub-channels. The demodulated symbol obtained on the  $k$ th sub-channel can thus be written as

$$Y_k = \frac{1}{\sqrt{N}} \sum_{n=0}^{N-1} y_n e^{-j2\pi kn/N}, \quad k = 0, 1, \dots, N-1. \tag{20}$$

If the CP is sufficiently longer than the CIR, then the ISI among OFDM symbols can be neglected. Therefore,  $Y_k$  can be reformulated as (Zhao & Huang, 1997; Hsieh & Wei, 1998)

$$Y_k = X_k H_k + I_k + W_k, \quad k = 0, 1, \dots, N-1, \tag{21}$$

where

$$\begin{aligned} H_k &= \sqrt{N} \sum_{i=0}^{M-1} \alpha_i e^{j\pi v_i T} \frac{\sin(\pi v_i T)}{\pi v_i T} e^{-j\frac{2\pi\tau_i}{N}k}, \\ I_k &= \frac{1}{\sqrt{N}} \sum_{i=0}^{M-1} \alpha_i \sum_{\substack{k'=0 \\ k' \neq k}}^{N-1} X(k') \frac{1 - e^{j2\pi(v_i T + k' - k)}}{1 - e^{j\frac{2\pi}{N}(v_i T + k' - k)}} e^{-j\frac{2\pi\tau_i}{N}k'}, \quad k = 0, 1, \dots, N-1 \end{aligned} \tag{22}$$

and  $\{W_k, k = 0, 1, \dots, N-1\}$  is the Fourier transform of  $\{w_n, n = 0, 1, \dots, N-1\}$ . The symbols  $\{Y_{p,k}\}$  received on the pilot sub-channels can be obtained from  $\{Y_k, k = 0, 1, \dots, N-1\}$ , the channel weights on the pilot sub-channels  $\{H_{p,k}\}$  can be estimated, and then the channel weights on the data (non-pilot) sub-channels can be obtained by interpolating or smoothing the obtained estimates of the pilot sub-channel weights  $H_{p,k}$ . The transmitted information-bearing symbols  $\{X_k, k = 0, 1, \dots, N-1\}$  can be recovered by simply dividing the received symbols by the corresponding channel weights, i.e.,

$$\hat{X}_k = \frac{Y_k}{\hat{H}_k}, \quad k = 0, 1, \dots, N-1, \quad (22)$$

where  $\hat{H}_k$  is an estimate of  $H_k$ . Eventually, the source binary data may be reconstructed by means of signal demapping.

### 3.2 Pilot sub-channel estimation

In the CTPA, the  $N_p$  pilot signals  $X_{p,m}$ ,  $m = 0, 1, \dots, N_p - 1$  are inserted into the FD transmitted symbols  $X_k$ ,  $k = 0, 1, \dots, N - 1$  with equal separation. In other words, the total  $N$  sub-carriers are divided into  $N_p$  groups, each of which contains  $Q = N/N_p$  contiguous sub-carriers. Within any group of sub-carriers, the first sub-carrier, with the lowest central frequency, is adopted to transmit pilot signals. The value of  $\rho = Q^{-1}$  denotes the pilot density employed in the OFDM communication studied here. The pilot density  $\rho$  represents the portion of the entire bandwidth that is employed to transmit the pilots, and it must be as low as possible to maintain sufficiently high bandwidth efficiency. However, the Nyquist sampling criterion sets a lower bound on the pilot density  $\rho$  that allows the CTF to be effectively reconstructed with a subcarrier-domain (i.e., FD) interpolation approach. The OFDM symbol transmitted over the  $k$ th sub-channel can thus be expressed as

$$X_k = \begin{cases} X_{mQ+l} \\ X_{p,m'} \\ \text{information} \end{cases} \quad \begin{cases} l = 0, \\ l = 1, 2, \dots, Q-1. \end{cases} \quad (23)$$

The pilot signals  $\{X_{p,m}, m = 0, 1, \dots, N_p - 1\}$  can either be a common complex value or sifted from a pseudo-random sequence.

The channel weights on the pilot sub-channels can be written in vector form, i.e.,

$$\mathbf{H}_p = \begin{bmatrix} H_p(0) & H_p(1) & \dots & H_p(N_p - 1) \end{bmatrix}^T \\ = \begin{bmatrix} H(0) & H(Q) & \dots & H((N_p - 1)Q) \end{bmatrix}^T. \quad (24)$$

The received symbols on the pilot sub-channels obtained after the FFT demodulation can be expressed as

$$\mathbf{Y}_p = \begin{bmatrix} Y_{p,0} & Y_{p,1} & \dots & Y_{p,N_p-1} \end{bmatrix}^T. \quad (25)$$

Moreover,  $\mathbf{Y}_p$  can be rewritten as

$$\mathbf{Y}_p = \mathbf{X}_p \cdot \mathbf{H}_p + \mathbf{I}_p + \mathbf{W}_p, \quad (26)$$

where

$$\mathbf{X}_p = \begin{bmatrix} X_p(0) & & & \mathbf{0} \\ & \ddots & & \\ & & & X_p(N_p - 1) \\ \mathbf{0} & & & \end{bmatrix},$$

$\mathbf{I}_p$  denotes the ICI vector and  $\mathbf{W}_p$  denotes the AWGN of the pilot sub-channels. In conventional CTPA-based CE methods, the estimates of the channel weights of the pilot sub-channels can be obtained by means of the LS CE, i.e.,

$$\begin{aligned} \hat{\mathbf{H}}_{LS} &= \left[ H_{p,LS}(0) \ H_{p,LS}(1) \ \cdots \ H_{p,LS}(N_p - 1) \right]^T \\ &= \left( \mathbf{X}_p^H \mathbf{X}_p \right)^{-1} \mathbf{X}_p^H \mathbf{Y}_p = \mathbf{X}_p^{-1} \mathbf{Y}_p \\ &= \left[ \frac{Y_p(0)}{X_p(0)} \ \frac{Y_p(1)}{X_p(1)} \ \cdots \ \frac{Y_p(N_p - 1)}{X_p(N_p - 1)} \right]^T. \end{aligned} \tag{27}$$

Although the aforementioned LS CE  $\hat{\mathbf{H}}_{LS}$  enjoys low computational complexity, it suffers from noise enhancement problems, like the zero-forcing equalizer discussed in textbooks. The MMSE criterion is adopted in CE and equalization techniques, and it exhibits better CE performance than the LS CE in OFDM communications assisted by block pilots (Van de Beek et al., 1995). The main drawback of the MMSE CE is its high complexity, which grows exponentially with the size of the observation samples. In a previous study (Edfors et al., 1996), a low-rank approximation was applied to a linear minimum-mean-square-error (LMMSE) CE assisted by FD correlation. The key idea to reduce the complexity is using the singular-value-decomposition (SVD) technique to derive an optimal low-rank estimation, the performance of which remains essentially unchanged. The MMSE CE performed on the pilot sub-channels is formulated as follows (Edfors et al., 1996):

$$\begin{aligned} \hat{\mathbf{H}}_{LMMSE} &= \mathbf{R}_{\hat{H}_{LS}\hat{H}_{LS}} \mathbf{R}_{H_p\hat{H}_{LS}}^{-1} \hat{\mathbf{H}}_{LS} \\ &= \mathbf{R}_{H_pH_p} \left( \mathbf{R}_{H_pH_p} + \sigma_w^2 \left( \mathbf{X}_p \mathbf{X}_p^H \right)^{-1} \right)^{-1} \hat{\mathbf{H}}_{LS}, \end{aligned} \tag{28}$$

where  $\hat{\mathbf{H}}_{LS}$  is the LS estimate of  $\mathbf{H}_p$  derived in Equation 27,  $\sigma_w^2$  is the common variance of  $W_k$  and  $w_n$ , and the covariance matrices are defined as follows:

$$\begin{aligned} \mathbf{R}_{H_pH_p} &= E \left\{ \mathbf{H}_p \mathbf{H}_p^H \right\}, \\ \mathbf{R}_{H_p\hat{H}_{LS}} &= E \left\{ \mathbf{H}_p \hat{\mathbf{H}}_{LS}^H \right\}, \\ \mathbf{R}_{\hat{H}_{LS}\hat{H}_{LS}} &= E \left\{ \hat{\mathbf{H}}_{LS} \hat{\mathbf{H}}_{LS}^H \right\}. \end{aligned}$$

It is observed from Equation 28 that a matrix inversion operation is involved in the MMSE estimator, and it must be calculated symbol by symbol. This problem can be solved by using a constant pilot, e.g.,  $X_{p,m} = c, m = 0, 1, \dots, N_p - 1$ . A generic CE can be obtained by averaging over a sufficiently long duration of transmitted symbols (Edfors et al., 1996), i.e.,

$$\hat{\mathbf{H}}_{LMMSE} = \mathbf{R}_{H_pH_p} \left( \mathbf{R}_{H_pH_p} + \frac{\beta}{\Gamma} \mathbf{I} \right)^{-1} \hat{\mathbf{H}}_{LS}, \tag{29}$$

where  $\Gamma = \frac{E\{|X_{p,k}|^2\}}{\sigma_w^2}$  is the average signal-to-noise ratio (SNR) and  $\beta = E\{|X_{p,k}|^2\}E\{|1/X_{p,k}|^2\}$  is a constant determined by the signal mapping method employed in the pilot symbols. For example,  $\beta = 17/9$  if 16-QAM is employed in the pilot symbols. If the auto-correlation matrix  $\mathbf{R}_{H_p H_p}$  and the value of the SNR are known in advance,  $\mathbf{R}_{H_p H_p} \left( \mathbf{R}_{H_p H_p} + \frac{\beta}{\Gamma} \mathbf{I} \right)^{-1}$  only needs to be calculated once. As shown in Equation 29, the CE requires  $N_p$  complex multiplications per pilot sub-carrier. To further reduce the number of multiplication operations, a low-rank approximation method based on singular-value decomposition (SVD) was adopted in the previous study (Edfors et al., 1996). Initially, the channel correlation matrix can be decomposed as

$$\mathbf{R}_{H_p H_p} = \mathbf{U} \mathbf{\Lambda} \mathbf{U}^H, \quad (30)$$

where  $\mathbf{U}$  is a matrix with orthonormal columns  $\mathbf{u}_0, \mathbf{u}_1, \dots, \mathbf{u}_{N_p-1}$ , and  $\mathbf{\Lambda}$  is a diagonal matrix with singular values  $\lambda_0, \lambda_1, \dots, \lambda_{N_p-1}$  as its diagonal elements. The rank- $\varrho$  approximation of the LMMSE CE derived in Equation 29 can thus be formulated as

$$\hat{\mathbf{H}}_{SVD} = \mathbf{U} \begin{bmatrix} \Delta_\varrho & 0 \\ 0 & 0 \end{bmatrix} \mathbf{U}^H \hat{\mathbf{H}}_{LS}, \quad (31)$$

where  $\Delta_\varrho$  denotes a diagonal matrix with terms that can be expressed as

$$\delta_k = \frac{\lambda_k}{\lambda_k + \frac{\beta}{\Gamma}}, \quad k = 0, 1, \dots, \varrho. \quad (32)$$

After some manipulation, the CE in Equation 31 requires  $2\varrho N_p$  complex multiplications, and the total number of multiplications per pilot tone becomes  $2\varrho$ . In general, the number of essential singular values,  $\varrho$ , is much smaller than the number of pilot sub-channels,  $N_p$ , and the computational complexity is therefore considerably reduced when the low-rank SVD-based CE is compared with the full-rank LMMSE-based CE derived in Equation 29. Incidentally, low-rank SVD-based CE can combat parameter mismatch problems, as shown in previous studies (Edfors et al., 1996).

### 3.3 Data sub-channel interpolation

After joint estimation of the FD channel weights from the pilot sub-channels is complete, the channel weight estimation on the data (non-pilot) sub-channels must be interpolated from the pilot sub-channel estimates. A piecewise-linear interpolation method has been studied (Rinne & Renfors, 1996) that exhibits better CE performance than piecewise-constant interpolation. A piecewise-linear interpolation (LI) method, a piecewise second-order polynomial interpolation (SOPI) method and a transform-domain interpolation method are studied in this sub-section.

**3.3.1 Linear interpolation**

In the linear interpolation method, the channel weight estimates on any two adjacent pilot sub-channels are employed to determine the channel weight estimates of the data sub-channel located between the two pilot sub-channels (Rinne & Renfors, 1996). The channel estimate of the  $k$ th data sub-channel can be obtained by the LI method, i.e.,

$$\hat{H}_{LI,x,k} = \hat{H}_{LI,x,mQ+l} = \left(1 - \frac{l}{Q}\right) \hat{H}_{x,m} + \frac{l}{Q} \hat{H}_{x,m+1}, \quad \begin{matrix} x = LS, LMMSE, SVD, \\ m = 0, 1, \dots, N_p - 2, \\ 1 \leq l \leq (Q - 1), \end{matrix} \quad (33)$$

where  $mQ < k = mQ + l < (m + 1)Q$ ,  $m = \lfloor \frac{k}{Q} \rfloor$ ,  $\lfloor \cdot \rfloor$  denotes the greatest integer less than or equal to the argument and  $l$  is the value of  $k$  modulo  $Q$ .

**3.3.2 Second-order polynomial interpolation**

Intuitively, a higher-order polynomial interpolation may fit the CTF better than the aforementioned first-order polynomial interpolation (LI). The SOPI can be implemented with a linear, time-invariant FIR filter (Liu & Wei, 1992), and the interpolation can be written as

$$\begin{aligned} \hat{H}_{SOPI,k} &= \hat{H}_{SOPI,x,mQ+l} \\ &= c_1 \hat{H}_{x,m-1} + c_0 \hat{H}_{x,m} + c_{-1} \hat{H}_{x,m+1}, \end{aligned} \quad (34)$$

where

$$\begin{aligned} x &= LS, LMMSE, SVD, & m &= 1, 2, \dots, N_p - 2, & 1 \leq l \leq (Q - 1), \\ c_1 &= \frac{\psi(\psi + 1)}{2}, & c_0 &= -(\psi - 1)(\psi + 1), & c_{-1} &= \frac{\psi(\psi - 1)}{2}, \\ \psi &= \frac{l}{N}. \end{aligned}$$

**3.3.3 Transform-domain-processing-based interpolation (TFDI)**

An ideal low-pass filtering method based on transform-domain processing was adopted for the data sub-channel interpolation (Zhao & Huang, 1997). In accordance with the CTPA, the pilot sub-channels are equally spaced every  $Q$  sub-channels. This implies that the coherence bandwidth of the multipath fading channel under consideration is sufficiently wider than the bandwidth occupied by  $Q$  sub-channels. After the pilot sub-channel estimation was completed, the interpolation methods mentioned in 3.3.2 and 3.3.3 were used to search for some low-order-polynomial-based estimations (say, LI and SOPI) of the channel weights of the data sub-channels. A transform-domain-processing-based interpolation (TFDI) method proposed in a previous study was used to jointly smooth/filter out the sub-channel weight estimates of the data sub-channels (Zhao & Huang, 1997). The TFDI method consists of the following steps: (1) first, it transforms the sub-channel weight estimates obtained from the pilot sub-channels into the transform domain, which can be thought of as the TD here; (2) it keeps the essential elements unchanged, which include at most the leading  $N_p$  (multipath) components because the coherence bandwidth is as wide as  $N/N_p$  sub-channels; (3) it sets the tail  $(N - N_p)$  components to zero; and (4) finally, it performs the inverse transformation

## Thank You for previewing this eBook

You can read the full version of this eBook in different formats:

- HTML (Free /Available to everyone)
- PDF / TXT (Available to V.I.P. members. Free Standard members can access up to 5 PDF/TXT eBooks per month each month)
- Epub & Mobipocket (Exclusive to V.I.P. members)

To download this full book, simply select the format you desire below

